Mining, Metallurgy & Exploration
https://doi.org/10.1007/s42461-025-01444-5

Recyclability Assessment and Design for Recycling Recommendations of End-of-Life NMC811 Lithium –Ion Batteries

Felipe Alejandro Garcia Paz[1] · Christine Nadine Prado Goerlach[2] · Chanchan Li[2] · Monika Keutmann[3] · Tobias Necke[2] · Mohsin Sajjad[1] · Karl Gerald van den Boogaart[1] · Ashak Mahmud Parvez[1]

Received: 14 July 2025 / Accepted: 2 December 2025

Abstract
This case study provides design for recycling (DfR) recommendations for NMC811 batteries, leveraging a detailed quantitative model of a recycling process optimized during the HydroLiBRec Research project. The adopted methodology integrated comprehensive empirical and analytical measurements to construct an accurate thermodynamic simulation of material and substance flow throughout the entire recycling process. This approach involved stages of manual dismantling, followed by hydro-mechanical, thermal treatment and hydrometallurgical processing of the end-of-life (EoL) NMC811 battery cells. Thermodynamic simulations were conducted using FactSage™ version 8.2 and HSC Chemistry 10 version 10.3.7.1 software to model the recovery of lithium present in the black mass via metallurgical processing methods. The results provided a detailed breakdown of the material composition post-dismantling, revealing that separated cells containing the active NMC811 material constituted 63.7% of the total weight. The study computes the recyclability index and quantify the recovery rates of individual elements, highlighting a recovery rate of 59.7% for lithium and an overall recycling index of 59.4%. The formatted data clearly supported material flow analysis and a product-centric approaches, which are crucial for optimizing DfR strategies and improving overall recycling efficiency. Recommendations included optimizing the dismantling process to achieve a 19% reduction in environmental impacts, such as Global Warming Potential (GWP), and avoiding the use of materials that would be lost in the recycling route. Overall, the measures are projected to increase the recycling index to 90%, thereby significantly improving the overall sustainability of the recycling process for NMC811 batteries. Moreover, a key finding highlighted the necessity of aligning product design with recycling process design in order to maximize recovery while minimizing impacts and losses.

Keywords Lithium-Ion battery · DfR · Hydromechanical recycling · Electrical vehicle · HSC sim · Life cycle assessment

1 Introduction

Lithium-Ion batteries (LIBs) are vital for modern energy storage, powering portable electronics, electric vehicles (EVs), and renewable integration. With high energy density, long cycle life, and declining production costs, LIBs now dominate markets from smartphones to grid storage systems [1] and are considered essential for the global transition to a low-carbon future [2]. Demand for LIBs is expected to grow significantly over coming decades, with lithium demand projected to rise several-fold by 2030–2050 under ambitious climate scenarios [3]. This surge, driven primarily by mobility and grid storage applications, highlighting dependence on critical raw materials (CRMs), notably lithium, cobalt, nickel, and manganese used in common cathode

✉ Ashak Mahmud Parvez
a.parvez@hzdr.de

[1] Helmholtz Institute Freiberg for Resource Technology (HIF), Helmholtz-Zentrum Dresden - Rossendorf e.V. (HZDR), Chemnitzer Straße 40, Freiberg 09599, Germany

[2] Fraunhofer Research Institution for Materials Recycling and Resource Strategies (IWKS), Aschaffenburger Straße 121, Hanau 63457, Germany

[3] Institute of Process Metallurgy and Metal Recycling, RWTH Aachen University, Intze Straße 3, Aachen 52056, Germany

Published online: 23 December 2025

chemistries such as NMC, NCA, and LCO [4]. The European Union classifies these elements as CRMs mainly due to supply chain vulnerabilities [5]. Their production is geopolitically concentrated: lithium from Chile, Argentina, and Australia; cobalt from the Democratic Republic of Congo; and battery-grade Class 1 nickel from China, Australia, and Indonesia [6, 7]. Graphite, used in anodes, is largely sourced from China and requires energy-intensive processing [6]. This reliance on limited number of suppliers raises concerns about long-term availability, price stability, and the environmental footprint of raw material extraction for LIBs.

To address these risks and reduce reliance on primary extraction, recycling of end-of-life (EoL) LIBs has become a strategic priority. Recycling enables the recovery of valuable metals, particularly lithium, cobalt, and nickel, for reuse in battery production, thereby supporting circular economy goals [8]. Life cycle assessment (LCA) studies show that raw material extraction dominates the most to LIBs environmental impacts [9, 10], while recycling can significantly reduce emissions, energy demand, and resource depletion. For instance, industrial-scale LCA based work indicates that recycling spent LIBs into battery-grade precursors can reduce greenhouse-gas emissions by over 58% compared to conventional mining [11]. Gaines et al. [12] found that closed-loop recycling can reduce energy use and emissions by over 50%, especially when powered by low-carbon electricity. Robust recovery of CRMs is therefore essential for building a sustainable and resilient battery supply chain.

In this context, Design for Recycling (DfR) has emerged as a powerful complementary strategy, which incorporates EoL considerations during product design to enable easier disassembly, material separation, and efficient recovery [13, 14]. For LIBs, researchers have identified a range of design variables such as adhesive types, cell formats, module architectures, and material homogeneity as critical to recyclability [3]. Moreover, DfR can also help reduce feedstock variability in recycling, which is crucial for the efficiency and safety of both mechanical and metallurgical processes. Nevertheless, implementing of these recommendations into practice can be challenging, as it may conflict with design goals such as maximizing energy density or minimizing cost. These trade-offs underscore the need for a life-cycle perspective, quantifying how upstream design decisions affect downstream recyclability and environmental performance. DfR is increasingly recognized as a key enabler of LIBs circularity. This paper systematically analyzes how design interacts with the recycling process, following established rules and guidelines. The goal is to derive DfR improvements with significant potential for enhancing recovery and process performance.

Recent research has begun integrating process modelling and environmental analysis to better inform LIBs recycling strategies. Using process simulation tools such as HSC Chemistry in combination with thermodynamic modelling and experimental data it is possible to predict the distribution of materials and energy across unit operations, offering realistic inputs for LCA models [15]. This approach ensures that emerging processes are evaluated using process-specific data rather than generic estimates [16, 17]. Multiple recent studies have leveraged such simulation-based LCAs to compare recycling routes (pyrometallurgical, hydrometallurgical, and direct regeneration) across different system boundaries and chemistries [18]. This combined methodology enhances the reliability of environmental assessments and clarifies the trade-offs associated with different recovery techniques.

Despite these advances, significant recycling challenges remain, such as the safe and efficient disassembly and sorting of batteries. In addition, EV battery modules are often sealed with adhesives, making manual separation laborious and hazardous [3]. Moreover, LIBs are present in diverse cell chemistries and formats, each requiring different recycling approaches. Inadequate sorting or feedstock heterogeneity can significantly reduce recovery yields [19]. Pyrometallurgical processes, although industrially established, have significant technical and environmental drawbacks. They require very high temperatures (> 1000 °C) to melt battery materials, making them extremely energy-intensive and producing large greenhouse gas (GHG) emissions [20]. Furthermore, they often fail to recover lithium effectively, as it tends to partition into slag [21, 22]. Hydrometallurgical routes operate at much lower temperatures and can offer better recovery for lithium and other metals but they depend on strong acids or bases and generate large volumes of secondary waste [9]. These methods involve multiple steps (such as shredding, leaching, solvent extraction and precipitation), making them complex and reagent-intensive; the spent reagents and effluents must be neutralized and treated, which increases cost and environmental burden [4, 20]. Direct recycling, which aims to regenerate cathode materials without breaking them down into elemental constituents, potentially saves energy, but it remains largely at the laboratory scale and is highly sensitive to feedstock purity and variability [18]. Small variations in residual impurities (binder, electrolyte, metal dust) can dramatically affect the chemical reprocessing needed to restore lithium content and electrochemical performance [23, 24]. As such, recycling technologies must balance recovery rates, recycling products quality, environmental performance, and cost-effectiveness, all of which are strongly influenced by initial product design and process choices.

While many studies focus on specific elements such as LCA, process simulation, or design principles, there remains a lack of integrated analysis that combines DfR,

Table 1 Composition of one Bosch power tube 500 e-bike battery packs (500 Wh) consisting of 40 NMC811 battery cells

Manual Dismantling		
Material	kg	wt.-%
Separated Cells	1.84776	63.7
Hard Plastic: Rubber, Insulation, Lid or Cover, Fastenings or Fixations, minimal contamination with metal/cables	0.42912	14.8
Plastic Cover	0.01733	0.6
Metal Fraction	0.07318	2.5
Casing (Aluminium)	0.5	17.2
Electronics	0.03418	1.2
Total	2.90	100

thermodynamic process simulation, and LCA, particularly for high-nickel chemistries like NMC811. In order to close this gap, these aforementioned methods were investigated in the HydroLiBRec project, which focused on an optimized process chain for the hydromechanical recycling of lithium-ion batteries in order to develop and optimize a highly efficient, economically viable, and environmentally friendly recycling route [25]. The overarching goal is to create the technological prerequisites for an effective, economically viable, environmentally friendly, and function-preserving battery recycling process. The present study briefly presents major findings from the HydroLiBRec project in order to demonstrate the challenge of sustainable lithium-ion battery recycling, with a strong emphasis on innovative hydromechanical and hydrometallurgical processes and integrating recyclability into battery design. Using dismantling experiments and hydromechanical pre-treatment data, we develop thermodynamic model via FactSage and HSC Sim to simulate the recycling process. These outputs are integrated into an LCA model to assess environmental impacts. The objective is to quantify material and energy flows, evaluate recovery efficiencies, and provide DfR recommendations that optimize critical material recovery while minimizing environmental burdens.

2 Materials and Methodology

In the current study, Bosch Power Tube 500 e-bike battery packs (capacity of 500 Wh) with a total weight of 2.9 kg and size of 36.0 × 6.5 × 8.3 cm (length x width x height) were chosen as input material. Manual disassembly of these packs resulted in 40 loose round cells (LG CHEM ING18650MJ1), which were then used for hydromechanical recycling activities. Specifically, this cell type was thoroughly selected as it contains widely used active material (NMC811, $LiNi_{0.8}Mn_{0.1}Co_{0.1}O_2$) and is generally challenging to recycle due to its comparatively robust steel casing [26]. Table 1 shows the composition of 40 cells pack NMC811 expended battery.

The initial step of optimizing the hydro-mechanical Li-Ion battery recycling system was to thoroughly analysis the material and substance flows, with a focus on the characteristics and composition of the recyclate fractions. As shown in Fig. 1, the block flow diagram includes essential pretreatment procedures, beginning with the manual dismantling of NMC811 battery pack from the 18,650 series. Afterwards, various mechanical, physical, and metallurgical processing units were employed in the recycling process. It is important to highlight that only the separated cell fraction was used

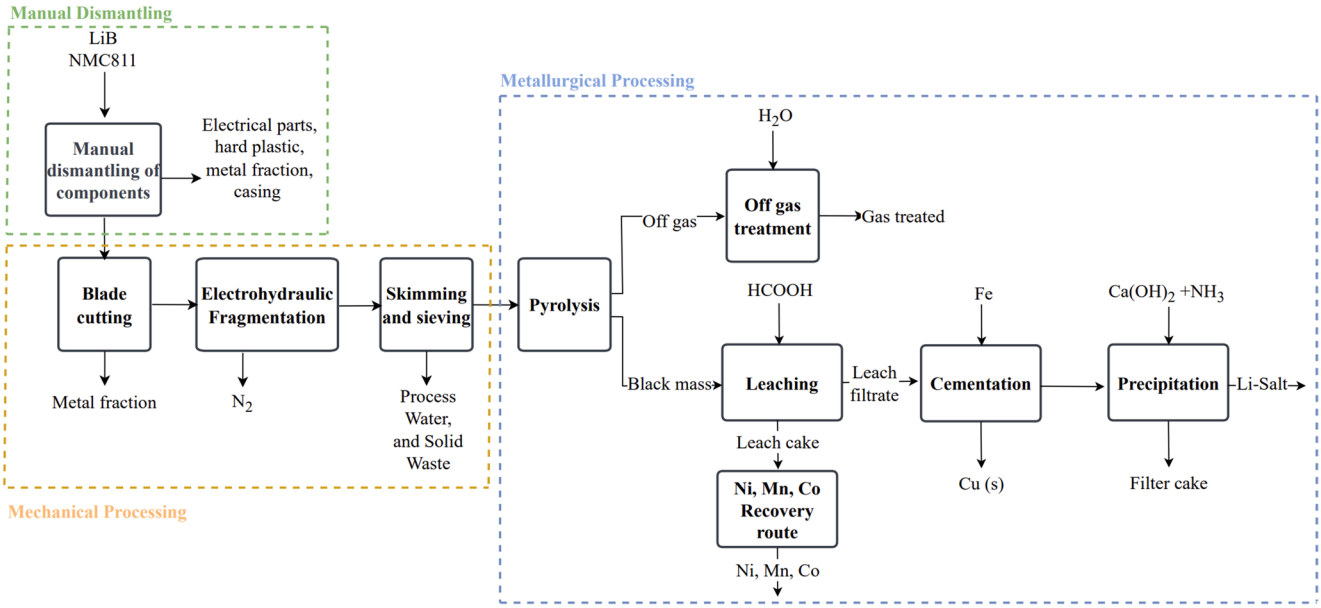

Fig. 1 Block flow diagram of recovery of lithium salt from LiB (NMC811)

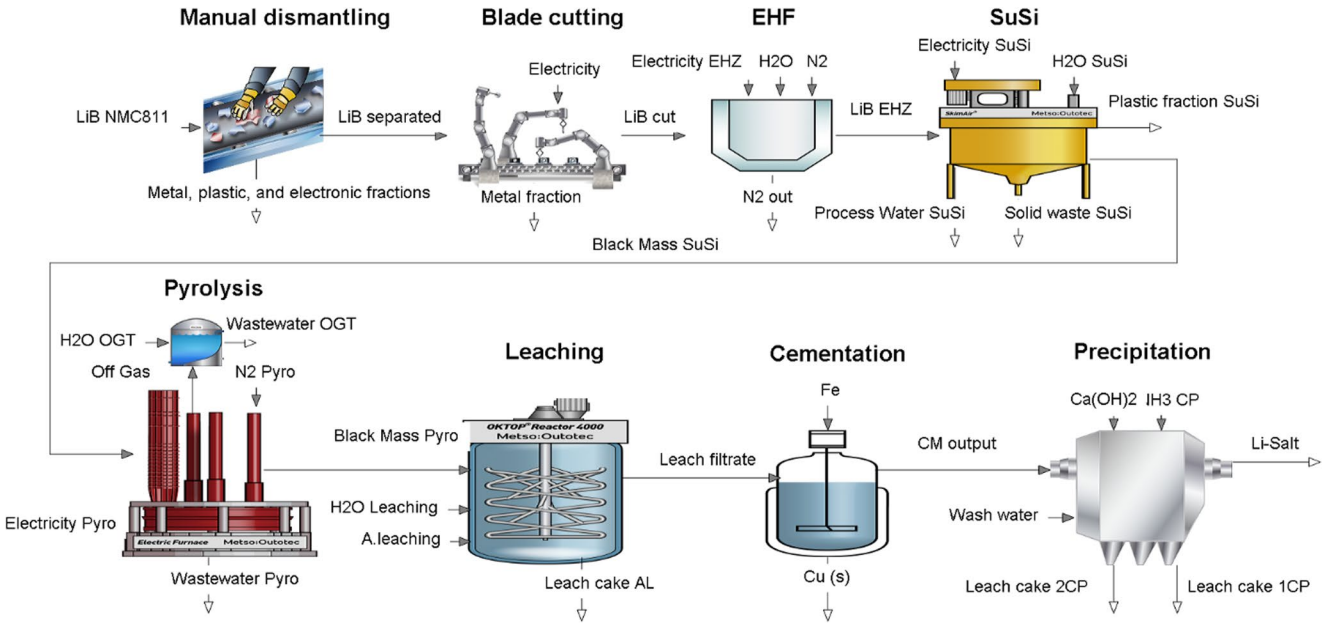

Fig. 2 HSC Simulation flowsheet for the investigated recycling process

Table 2 Input material including cell components and their chemical compositions

Input EHF			
Cell Component	Composition	Kg	[wt%]
Anode	Cu	0.070	6.98
Anode	C	0.254	25.31
Cathode	Al	0.050	4.95
Cathode-Active Material NMC 811	Li	0.025	2.50
	Ni	0.169	16.88
	Mn	0.020	1.98
	Co	0.021	2.12
	O	0.115	11.51
Cathode Binder PVDF fluoropolymer	$C_2H_2F_2$	0.030	2.99
Case-Steel	Fe	0.055	5.50
	Ni	0.029	2.91
Extra-Element in Off-Gas and Black Mass	B	0.0001	0.01
	S	0.001	0.06
	Ca	0.001	0.13
	Mg	0.0002	0.02
	Na	0.00004	0.00
	Si	0.003	0.32
Separator foil	C_2H_4	0.019	1.84
Elektrolyt, org. Carbonate	$LiPF_6$	0.028	2.80
	$C_3H_4O_3$	0.028	2.80
	$C_4H_6O_3$	0.028	2.80
	$C_3H_6O_3$	0.028	2.80
	$C_5H_{10}O_3$	0.028	2.80
Total		1.00	100
Water	H_2O	14.41	
N_2	N_2	1.14	
Total		16.556	

as input for the subsequent processing units. The plastics, metal fraction, casing, and electronics listed in Table 1 were discarded after dismantling and were thus not subjected to further elemental characterization.

Following the recycling pathway shown in Fig. 2, the process started with a physical processing unit including blade cutting to weaken the housing of the battery cell, in order to facilitate the detachment of the cell and the delamination of the anode and cathode foils. Next, the electrohydraulic fragmentation (EHF) technique was applied, followed by skimming and sieving (SuSi), yielding an intermediate product known as black mass. This black mass was then subjected to pyrolysis before undergoing a series of hydrometallurgical treatments including leaching, cementation, and precipitation in order to produce a lithium salt as the final product. The thermodynamic simulation model was developed using HSC Chemistry version 10.3.7.1 and FactSage™ version 8.2. This model offers critical insights for applying DfR principles throughout this process.

For the thermodynamic simulation, accurate material flow and elemental composition are essential. This requires data from both empirical measurements using analytical measurements such as Inductively Coupled Plasma - Optical Emission Spectroscopy (ICP-OES) and X-Ray Diffraction (XRD) analysis and thermodynamic calculations, provided by FactSage. Table 2 presents the weight% composition following manual dismantling, which provides a detailed breakdown of components obtained from the manual dismantling of NMC811 LIBs, which is crucial for understanding material distribution and potential recovery.

Among these components, the separated cells constitute the largest share at 63.7%, which contains exclusively the targeted NMC811 active material. This fraction will be the only considered for the hydromechanical LIBs recycling system simulation. Additionally, hard plastic and rubber insulation account for 14.8%, while the plastic cover represents a minor component at 0.6%. The metal fraction comprises 2.5%, potentially including small metallic parts suitable for separate recycling routes. The aluminum casing is a significant material, making up to 17.2% of the total. Electronics represent the smallest fraction (around 1.2%), which may include further valuable metals for further recycling activities.

2.1 Blade Cutting

The detached cell, acquired post-manual dismantling, required thorough characterization of its elemental composition, encompassing the anode, cathode, casing, and electrolyte components within the battery cell, quantified in both mass and weight%. Subsequently, the cutting process was conducted at Fraunhofer IWKS (Germany) with the objective of facilitating the detachment and liberation of the casing of the NMC811 battery cell. The blade cutting procedure was executed twice at front and back site of the battery cell to enhance the liberation efficiency during EHF treatment. Material losses in this step were limited to casing components, with iron and nickel exhibiting losses of 1.79% and 3.33%, respectively. Crucially, the core LIB components, including the essential NMC elements, remained unaffected.

2.2 Electrohydraulic Fragmentation

An EHF system (EHF-400, ImpulsTec GmbH, Germany) was selected for producing NMC black mass as an intermediate product before hydrometallurgical processing. In this EHF process, 30 round cells per batch were processed in a stainless-steel reactor with shock waves in 20 l of water at a voltage of 40 kV and a frequency of 1.5 Hz in order to open the cells and detach anode and cathode powders from the metal foils. This procedure was then repeated until all batteries had been successfully disassembled, which necessitates 1500 to 2000 pulses at the given setting. The process and methodological details can be found elsewhere [27, 28].

The aforementioned procedure was designed to separate and delaminate composite materials such as anode or cathode foils found in the spent NMC811 battery cell. The intense electrical discharges induce shock waves that mechanically fragment cells and delaminate anode and cathode powders from metal foils, selectively separating materials for subsequent SuSi. The outputs from the EHF process were then managed in the subsequent SuSi process. For the material flow analysis (as detailed in Table 2), it was assumed that no losses has been occurred at this particular process.

2.3 Skimming and Sieving

After the EHF process, the intermediate fractions underwent further refinement through SuSi. This water-based process was meticulously designed to segregate materials based on their particle size and specific density. The EHF output was thus separated into multiple value-added fractions in one process unit, and black mass was recovered as an intermediate product.

During SuSi procedures, the wet mixture of fragmented cell-materials including black mass, casings, anode, cathode and separator foils were treated in a hydro cyclone device. In this stage, the light fraction, especially the separator plastics floats to the surface of the processing water, allowing it to be skimmed off. At the same time, the heavier fractions were settled at the bottom, where a 500 µm sieve separates the black mass (fine fraction) from the metal parts (coarse fraction). A key advantage of this treatment is the individual recovery and recycling of several value-adding intermediate products: plastics, coarse metals (including steel housings, aluminium, and copper foils), and black mass. For this work, only the fine-grained black mass was relevant because it's significantly enriched with critical metals like lithium. As shown in Fig. 3, losses can be quantified in graphite from the anode, as well as in iron and nickel from the casing material. Additionally, losses are noted in the separator foil and organic carbonates.

2.4 Pyrolysis

Pyrolysis is a key step in the recycling process of NMC 811 spent batteries, as it enables the thermal decomposition of organic components such as binders and electrolytes in the absence of oxygen, thereby minimizing the formation of GHG typically associated with combustion. Specifically, in the context of recycling, pyrolysis facilitates the disassembly of the chemical complex structure, effectively segregating organic materials from inorganic components [29]. This process was conducted at IME (RWTH University, Germany) at a temperature of 500 °C in a resistance-heat furnace under N_2 environment. The methodology involved comprehensive analysis of both input and output products through various techniques such as ICP-OES (as shown in Table 3) and XRD analysis (as presented in Table 4). Additionally, the process was simulated using FactSage, providing empirical data shown in Table 5 for comparative analysis. The aim of this comparative analysis was to

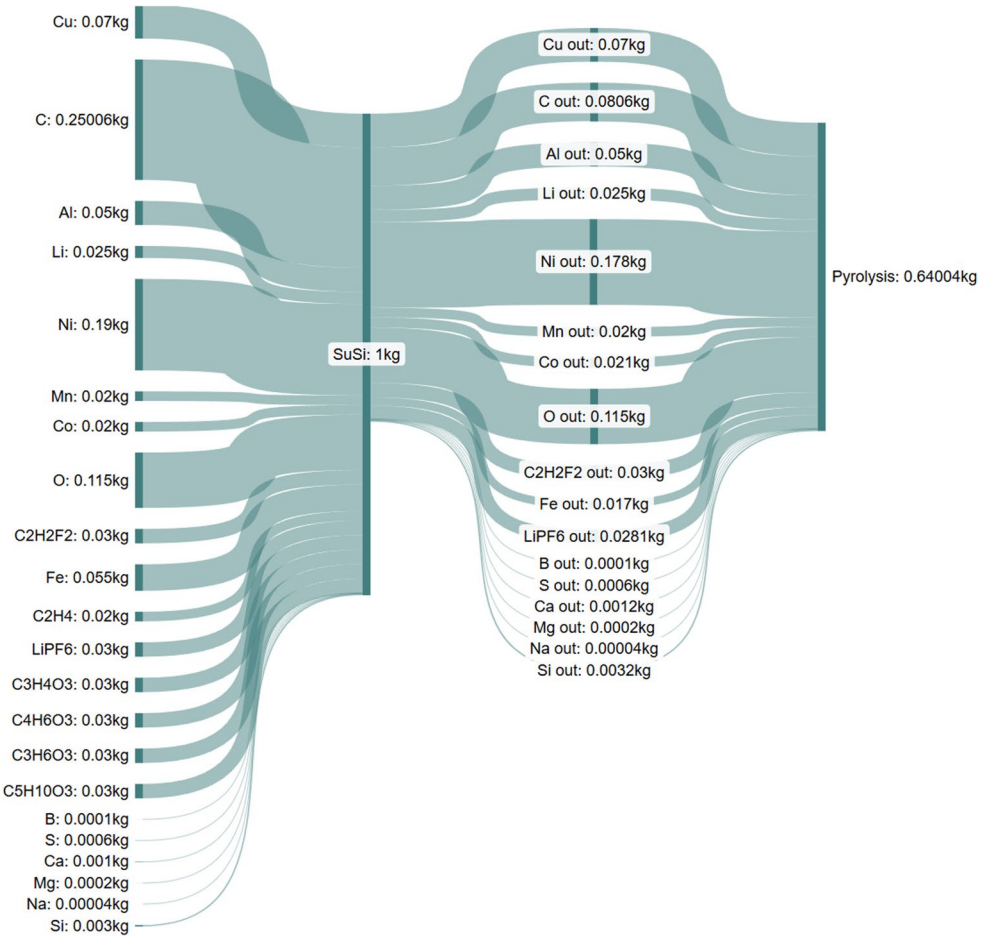

Fig. 3 Sankey diagram of the material flows during the SuSi process following EHF. The figure visualizes how the fragmented cell materials are separated in a water-based hydrocyclone system according to particle size and density

Table 3 Chemical composition in wt% of the black mass obtained by EHF treatment after SuSi and after additional pyrolysis at 500 °C for 120 min

Al	B	Ca	Co	Cu	Fe	Li
2.581	0.011	0.129	3.922	3.674	1.453	3.719
Mg	Mn	Na	Ni	S	Si	Insoluble
0.024	1.42	0.004	32.633	0.062	0.323	36.33

Table 4 Semi-quantitative XRD analysis (wt%) of black mass following pyrolysis at 500 °C for 120 min

Phases and their chemical Composition	wt%
Lithium Nickel Manganese Cobalt Oxide ($Li_1Ni_{0.75}Mn_{0.1}Co_{0.15}O_2$)	27
Copper (Cu)	3
Zabuyelite (Li_2CO_3)	8
Paramelaconite (Cu_4O_3)	1
Nickel Oxide (NiO)	6
Nickel (Ni)	7
Graphite 3R (C)	48
Total	100

elucidate the composition of various phases present in the resulting black mass post-pyrolysis, which will undergo subsequent leaching. For instance, as shown in Fig. 4, copper, initially present at 0.070 kg or 10.94%, undergoes transformations into different states such as Cu (0.067 kg, 10.98%), Cu_4O_3 (0.003 kg, 0.4%) and Cu_2S (0.001 kg, 0.1%). Lithium undergoes transformations into compounds such as Li_2CO_3 (0.021 kg, 3.5%) and LiF (0.038 kg, 6.23%), among others. Notably, this process resulted in a reduction in total mass from 0.640 kg to 0.609 kg in the black mass output, reflecting the efficiency of material recovery and transformation, with the remaining mass accounted for as off-gas, and losses.

2.5 Formic Acid Leaching

For black mass recycling, the initial hydrometallurgical step involves a leaching process conducted at 70 °C, based on parameters provided by IME. In this methodology, a mixture of formic acid and water enables the dissolution of valuable elements from the black mass. The interaction between the black mass and formic acid initiates chemical reactions that

Table 5 Empirical data in (wt%) obtained through factsage

Al	Al_2O_3	B	C	C_graphite
3.12E-23	0.001622	2.16E-18	0.001191	0.235822138
Ca	CaO	$CaMg_2Al_{16}O_{27}$	CaF_2	Co
4.39E-25	3.01E-06	0.000354	0.001528	0.01222175
CoO	Co_fcc	Cu	CuO	Cu_fcc
0.000182	0.036272594	0.000163	1.50E-09	0.154382
Cu_2S	Fe	FeO	Fe_2O_3	Li
0.005427	0.023262547	0.014927	0.000203632	2.45E-18
Li_2O	$LiAlO_2$	LiF	$LiAl_5O_8$	Li_3PO_4
1.38E-10	0.012674	0.031939	0.003037884	0.008803
Li_2SiO_3	Mg	MgO	Mn	MnO
0.003614549	9.04E-20	2.81E-05	8.29E-08	0.045247
Na	Na_2O	$Na_2Ca_3Al_{16}0_{28}$	Ni	NiO
1.75E-25	1.85E-18	9.14E-05	0.027979	5.03E-06
Ni_fcc	P	Si		
0.37902	2.24E-15	6.03E-18		

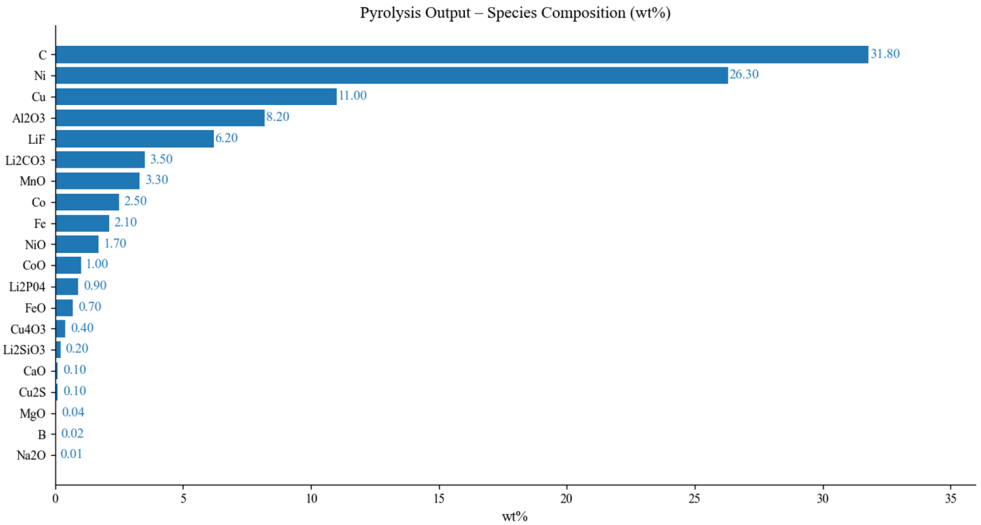

Fig. 4 Species distribution in the pyrolysis output expressed in wt%. The bar chart shows the relative contribution of each compound after thermal treatment. Carbon (31.8 wt%), nickel (26.3 wt%), and copper (11.0 wt%) are the most abundant constituents, followed by lithium fluorides and carbonates. Minor oxides and trace elements are also included to fully represent the chemical composition of the recovered solid fraction

lead to the formation of formate salts, such as lithium formate, iron formate, and copper formate (as shown in Table 6). Table 7 presents the leaching yields obtained by IME. HSC Sim modeling was employed to evaluate the theoretical recovery based on equilibrium calculations under the defined process conditions, given that the leaching environment had already been experimentally established and the use of this acid has been documented in previous studies [30–32]. In this process, the nickel, manganese, and cobalt remaining in the filter cake require hydrothermal treatment to enable their recovery and regeneration for reuse as active cathode materials. Although this downstream recovery step was not simulated in the present study, the theoretical recovery has been considered.

2.6 Precipitation

After leaching but before precipitation, copper is recovered in the cementation process unit. However, due to the absence of experimental data for process parameters, this step was not simulated. Instead (as shown in Table 8), the recovery of Cu was assumed based on the amount of copper in the leach filtrate as determined by the copper leaching yield.

This stage initiated a series of chemical reactions that culminate in the formation of solid outputs, including waste. As a last step the water was removed by evaporation, and the lithium salt was obtained. The chemically balanced reactions and resulting products shown in Table 9 were generated using equilibrium simulations in HSC Sim, where the reaction progress was adjusted to obtain a final lithium salt composition consistent with the ICP-OES results reported by ISC Fraunhofer in Table 10.

3 Life Cycle Assessment

The objective of this comprehensive gate to gate LCA was to conduct a detailed quantitative evaluation of the environmental impacts associated with the recycling process

Table 6 Post-leaching reaction products and pathways resulting from the hydrometallurgical process using formic acid, modeled using HSC Sim

Filtrate	kg	wt%
$Al(CHOO)_3$	0.014	0.005
$B(CHO_2)_2$	0.0001	0.00004
$C+H_2O$	2.55	0.97
$Ca(CHO_2)_2$	0.001	0.0003
$Co(CHO_2)_2$	0.0002	0.0001
CoF	0.0002	0.0001
$Cu(CHO_2)_2$	0.013	0.005
$Fe(CHO_2)_2$	0.003	0.001
LiCHOO	0.041	0.015
$Mg(CHO_2)_2$	0.0002	0.0001
$Mn(CHO_2)_2$	0.002	0.001
$Ni(CHO_2)_2$	0.005	0.002
Total	2.63	1
Filter Cake	kg	wt%
Nickel Formate Hydrate $Ni(HCOO)_2(H_2O)_2$	0.194	23.054
Cobalt Formate Hydrate $Co(HCOO)_2(H_2O)_2$	0.021	2.473
$C+H_20$	0.457	54.232
Manganese Hydroxide Oxide Mn(OH)O	0.018	2.107
Copper Formate Hydrate $Cu(CHO_2)_2(H_2O)_2$	0.057	6.704
xAl_2O_3	0.036	4.261
FeO	0.014	1.655
Lithium Formate Hydrate $Li(HCOO)_2(H_2O)_2$	0.026	3.041
Cobalt Oxide CoO	0.021	2.473
Total	0.843	100

Table 7 Leaching yield data obtained by IME using formic acid as the leaching agent

Element	Leaching yield %
Al	27.72
Co	1.97
Cu	19.26
Fe	16.97
Li	61.31
Mn	10.39
Ni	2.66

Table 8 Product resulting from the cementation process in wt%

Filtrate	Kg	wt%
$Al(CHOO)_3$	0.0138	0.0052
$B(CHO_2)_2$	0.0001	0.00004
$C+H_2O$	2.5502	0.9697
$Ca(CHO_2)_2$	0.0009	0.0003
$Co(CHO_2)_2$	0.0002	0.0001
CoF	0.0002	0.0001
$Fe(CHO_2)_2$	0.00001	0.00001
$Cu(CHO_2)_2$	0.0029	0.0011
$Mn(CHO_2)_2$	0.0406	0.0154
$NaCHO_2$	0.0002	0.0001
$Ni(CHO_2)_2$	0.0021	0.0008
Total	2.63	1
Cementation Cake	Kg	
Cu (s)	0.013	

Table 9 Chemically balanced reactions and products generated during the precipitation process, modeled using HSC sim software

Precipitation output (Li salt)		
Filtrate	kg	wt%
$B(CHO_2)_2$	0.00015	0.05
$Ca(CHO_2)_2$	0.18586	60.76
$Co(CHO_2)_2$	0.00003	0.01
$Cu(CHO_2)_2$	0.00001	0
$Fe(CHO_2)_2$	0.00014	0.05
LiCHOO	0.11780	38.51
$Mg(CHO_2)_2$	0.00002	0.01
$Mn(CHO_2)_2$	0.00005	0.02
$NaCHO_2$	0.00087	0.29
$Ni(CHO_2)_2$	0.00019	0.06
Total	0.3059	1
(Calcium hydroxide) flouride precipitation output		
Precipitation Cake 1	kg	wt%
$Al_3(PO_4)_2(OH)_3*5H_2O$	0.0048	2.83
$MnAl_2(PO_4)_2(OH)_2*6H_2O$	0.0048	2.83
$*3CaO*Al_2O_3*Ca(OH)_2*18H_2O$	0.0048	2.83
$Ca(CO)_3$	0.0048	2.83
CoF_3	0.0014	0.85
NiO*OH	0.0048	2.83
$H_2FeAl(PO_4)_6(OH)_8*16(H_2O)$	0.0048	2.83
$Ca(OH)_2$	0.0048	2.83
Total	0.1686	1
(Ammonia) mixed hydroxide precipitation output		
Filtrate	kg	wt%
C	4.05E-05	3
$CaCO_3$	0.0012	89
$NaMnFeO_2$	0.000108	8
Total	0.00135	100

Table 10 ICP-OES analysis of lithium salt in wt%

B	Ca	Co	Cu	Fe	Li
0.048	60.762	0.010	0.005	0.047	38.513
Mg	Mn	Na	Ni	S	Si
0.008	0.016	0.285	0.063	0.179	0.066

of NMC811 battery cells. The main function of the evaluated recycling process is the treatment of the LIBs. Consequently, the functional unit for this assessment is defined as the treatment of 1 kg of used NMC811 battery cells, serving as the basis for evaluating the efficiency and environmental performance of the process. Simultaneously, the recycling process targets to recover the active materials, especially lithium, present in the cathode of the NMC811 battery. Therefore, the LCA results were focused on the recycling of LIBs, with the recovered lithium salt as the only system product. Figure 4 illustrates the system boundary, which include all the inputs (resources required for recycling) and outputs (emissions, waste and product) (Fig. 5).

In this study, the environmental assessment incorporates both foreground and background data to ensure a comprehensive analysis of the recycling process. The foreground data,

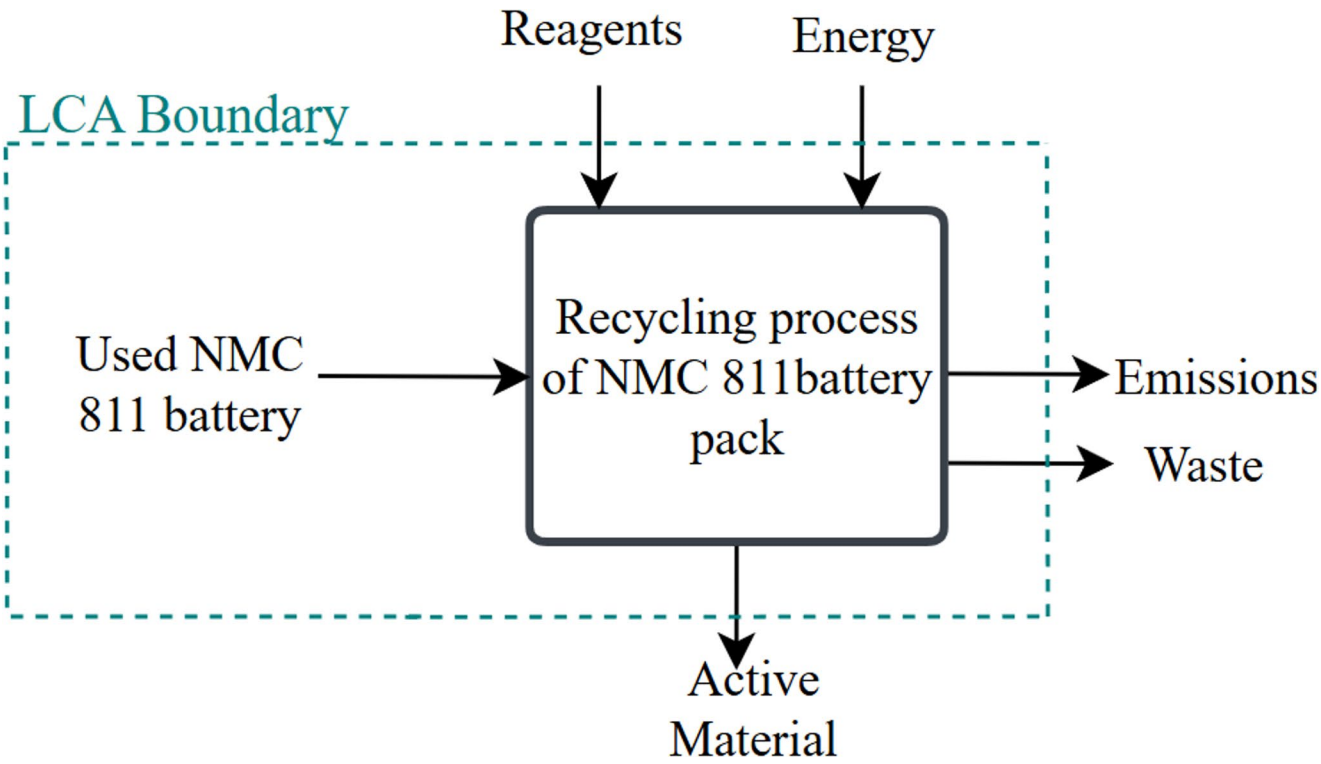

Fig. 5 LCA system Boundary

obtained from pilot-scale operations conducted at Hydro-LiBRec Project, include a comprehensive quantification of reagents and materials consumed, energy requirements in terms of electricity usage, and detailed characterization of intermediate products. The latter was achieved through advanced analytical techniques, specifically XRD and ICP-OES, ensuring a precise and robust dataset for the assessment. For the background data, the Ecoinvent v3.8 [33] database was utilized, providing a robust and reliable foundation for the Life Cycle Inventory (LCI).

In the absence of background data, process simulation was employed as a complementary approach to compile foreground LCI data and assess the environmental impacts throughout the entire recycling process. The aforementioned methodology, extensively validated in prior studies [34, 35] facilitated the estimation of critical simulation parameters such as process conditions, reagent concentrations, and yields. These parameters were sourced from laboratory-scale literatures or extrapolated through expert-informed estimations based on comparable hydrometallurgical processes [36, 37].

In the present study, the EF 3.0 method was applied for the LCA, with a hierarchist perspective, to perform the LCIA [38]. This methodology, developed by the European Commission's Joint Research Centre (JRC) provides a harmonized and science-based approach for assessing environmental performances. It is grounded in the ISO14040/14,044 standards for LCA, and evolved from the earlier International Life Cycle Data System (ILCD) framework by revising and updating many LCA methods but focuses exclusively on midpoint indicators. In this study, impact scores at midpoint level were calculated for the following impact categories: Global Warming Potential (total) (GWP100, kg CO_2-eq.), Acidification Potential (AP, mol H+-eq.), Human Toxicity Potential (HTP, kg 1,4-DCB-eq.), Eutrophication (freshwater) Potential (EP, kg P-eq.), and Abiotic resource depletion - minerals and metals (ADP, kg Sb-eq).

4 Design for Recycling

Design for Recycling (DfR), a central strategy in Eco-design, employs a comprehensive set of technical considerations throughout product development to maximize the efficient recovery of materials from EoL product [39, 40]. Moreover, DfR rules and guidelines' provide designers and engineers with principles and best practices (such as material selection, modular design, minimizing toxicity, and simplifying assembly) to create end-of-life products that are easier to recycle, leading to simplified disassembly, enhanced material recovery, and improved overall sustainability [41]. As emphasized in [42] a product-centric recycling methodology extends beyond basic disassembly and physical recycling (e.g. material separation) by integrating

with metallurgical processes and other end-stage treatment methods. This phase closes the loop by returning recovered materials to the resource cycle for more sustainable use. The Recycling Index is therefore a critical metric for measuring recycling performance [43]. It is calculated by dividing the recovery rate of individual elements by their total input, providing a detailed evaluation of sustainability. This metric reinforces the importance of adopting a product-centric recycling framework.

Design for Resource Efficiency (DfRE), which includes DfR as a component, requires an understanding of material liberation behaviour, the particulate quality of recyclates, and the efficiency of separation processes. This includes assessing the compatibility of materials and their recovery or loss during metallurgical processing. These factors must be modelled and evaluated based on design decisions, connection types, and the materials used in the product.

Eco-labeling, within the framework of DfR, is the practice of certifying products with labels that communicate their environmental qualities, including ease of recycling and general eco-friendliness [44] Ecolabels offer consumers and stakeholders clear, standardized information regarding a product's environmental performance throughout its entire lifecycle.

5 Results and Discussion

As illustrated in Fig. 6, the Sankey diagram provides a comprehensive overview of the weight and distribution of materials throughout each stages of the recycling process, leading to the extraction of lithium salt from NMC811 LIBs. This analysis tracks the flow of materials from the initial dismantling and processing of battery components, through mechanical and metallurgical treatments, until the final recovery of lithium salt. By allocating recovered metals on a mass basis and conducting a detailed process examination, we were able to quantify material losses and efficiencies at every stage, revealing opportunities for optimization.

The thermodynamic simulations are based on equilibrium models. Accordingly, the reported recovery rates represent theoretical potentials rather than industrial performance, as variability may arise from feed composition, reagent ratios, process temperatures, and leaching yields. Although a full sensitivity analysis was beyond the scope of this study, the coherence of model outputs with expected process behavior supports the robustness of the observed trends. It is therefore necessary for future research to include a systematic sensitivity assessment that quantifies the influence of key parameters on recovery efficiency and environmental impacts.

5.1 Recyclability Index and Eco Labeling of Products

The Recycling Index is a crucial metric for assessing the effectiveness of recycling, both for products and their constituent materials. This index is derived by calculating the recovery rate of individual elements relative to their total weight, providing a detailed evaluation of their sustainability impact. This underscores the importance of adopting a product-centric approach to recycling.

As demonstrated in Table 11, comprehensive elemental weights of the Battery cell NMC811 were meticulously evaluated both before and after undergoing the recycling process. This assessment allowed for the determination of recovery rates. In accordance with proposals by [45], and as

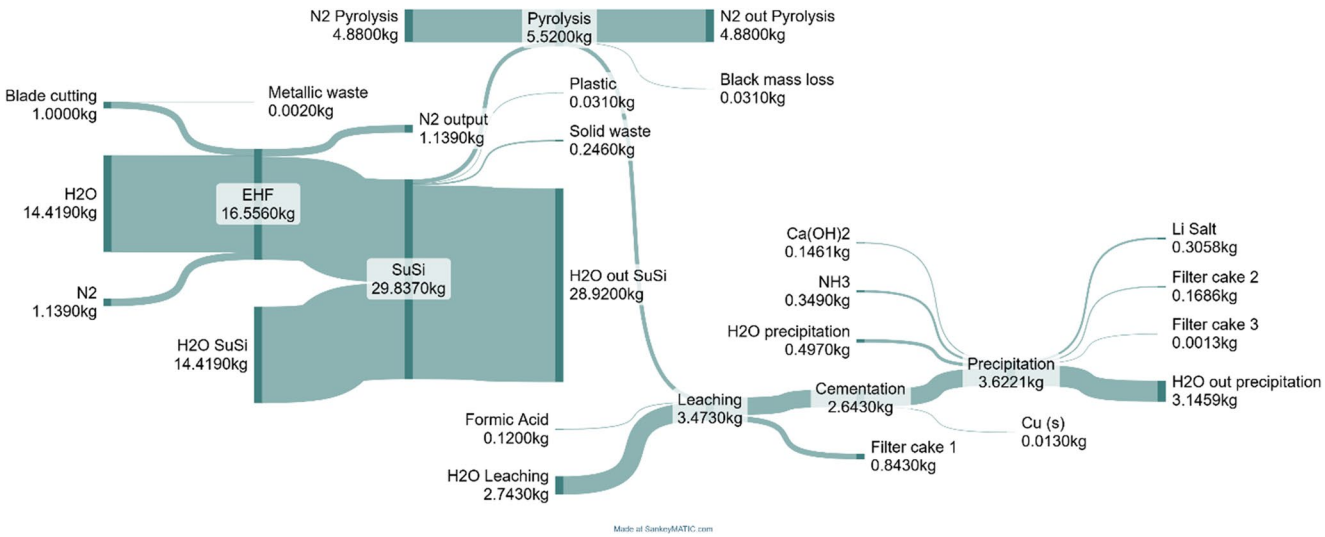

Fig. 6 Sankey diagram of material flows in NMC811 LIB recycling, combining black mass production and hydrometallurgical leaching and precipitation

Table 11 Recyclability index from a product perspective showing the overall recovery rate of all elements within the NMC811 battery cell

Element	Weight in Battery Cell (kg)	Recovery weight	Recovery Rate
Cu	0.07	0.013	19.24
C	0.396	0.228	57.49
Al	0.05	0	0
Li	0.026	0.016	59.79
Ni	0.2	0.194	97.34
Mn	0.02	0.018	89.61
Co	0.021	0.021	98.03
Fe	0.056	0.038	68.3
P	0.006	0	0
F	0.04	0	0
Total	0.888	0.528	59.468

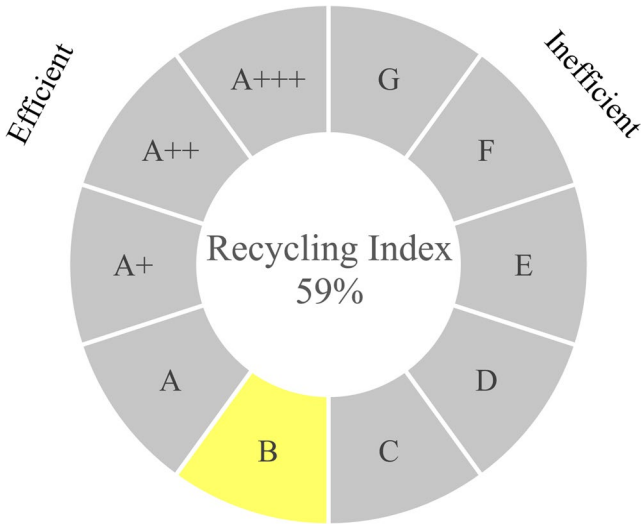

Fig. 7 Recycling Efficiency Label for NMC 811 Battery Cell

shown in Fig. 7, leveraging this data could enable the development of a product label that effectively communicates its recycling efficiency or inefficiency. Such labeling not only enhances consumer awareness but also promotes sustainable practices across the lifecycle of products.

To contextualize the obtained recovery performance within the broader field of lithium-ion battery recycling, a comparative analysis was conducted using literature data for other cathode chemistries such as LFP, NMC111, and LCO. The recyclability index derived in this study (59.4%) represents a mass-weighted aggregation of the element-specific recovery rates reported in Table 11. Recent studies indicate that optimized hydrometallurgical systems for LFP batteries can achieve lithium recoveries above 90%, with almost complete recovery of iron and phosphate fractions [4, 9]. Similarly, NMC111 chemistries commonly report lithium recovery between 80 and 95%, whle nickel and cobalt recoveries exceeding 95% [36, 37], nd manganese recovery remains close to 90%. For LCO cahodes, recoveries of both lithium and cobalt typically reach 90–98% [12].

In contrast, the lithium recovery in the present NMC811 system (≈60%) is lower than these optimized benchmarks, while the transition-metal recoveries (nickel, cobalt, manganese) remain within a comparable range. This difference arises mainly from the use of formic acid as an environmentally benign leaching reagent, which provides lower dissolution kinetics than strong inorganic acids such as H_2SO_4 or HCl. Furthermore, the modeled process chain excluded delamination and flotation steps, resulting in incomplete liberation. The primary goal of this work was to establish a design-for-recycling assessment framework based on thermodynamic modeling and life-cycle analysis, rather than to optimize the leaching performance. As mentioned earlier, adding a delamination stage could raise the overall recyclability from 59% to 71%, and further process optimization may enhance recovery yields while maintaining environmental compatibility.

5.2 Results Based on Rules and Guidelines

These rules and guidelines, provided by [42] establish a comprehensive framework for the DfR of EoL NMC811 LIBs. Accordingly, the following considerations have been made:

a) **Product-specific and recycling system-specific**: As shown in Fig. 1, the designated recycling route, integrating mechanical, physical, and chemical processes, has been meticulously customized for the NMC811 battery cell, thereby establishing a distinctive recyclability profile. This approach encompasses the efficient recovery of lithium salt as a final product, while also prioritizing the extraction of other valuable materials as intermediate products.

b) **Model and simulation quantification**: As shown in Fig. 2, the material and substance flow analysis was developed using HSC Sim, while the equilibrium mode for pyrolysis was done using FactSage. The integration and computation of this information enable us to establish a robust simulation model.

c) **Data in a consistent format**: The generated data has been meticulously presented in both weight (wt) and weight% (wt%) formats to facilitate clear comprehension of material flow dynamics. This approach ensures that stakeholders involved in the DfR process for the NMC811 battery cell can easily access and utilize the information. By integrating these detailed metrics, the material flow throughout the recycling process becomes transparent, allowing for informed decision-making and optimization of recycling strategies. The dataset is accessible under [46].

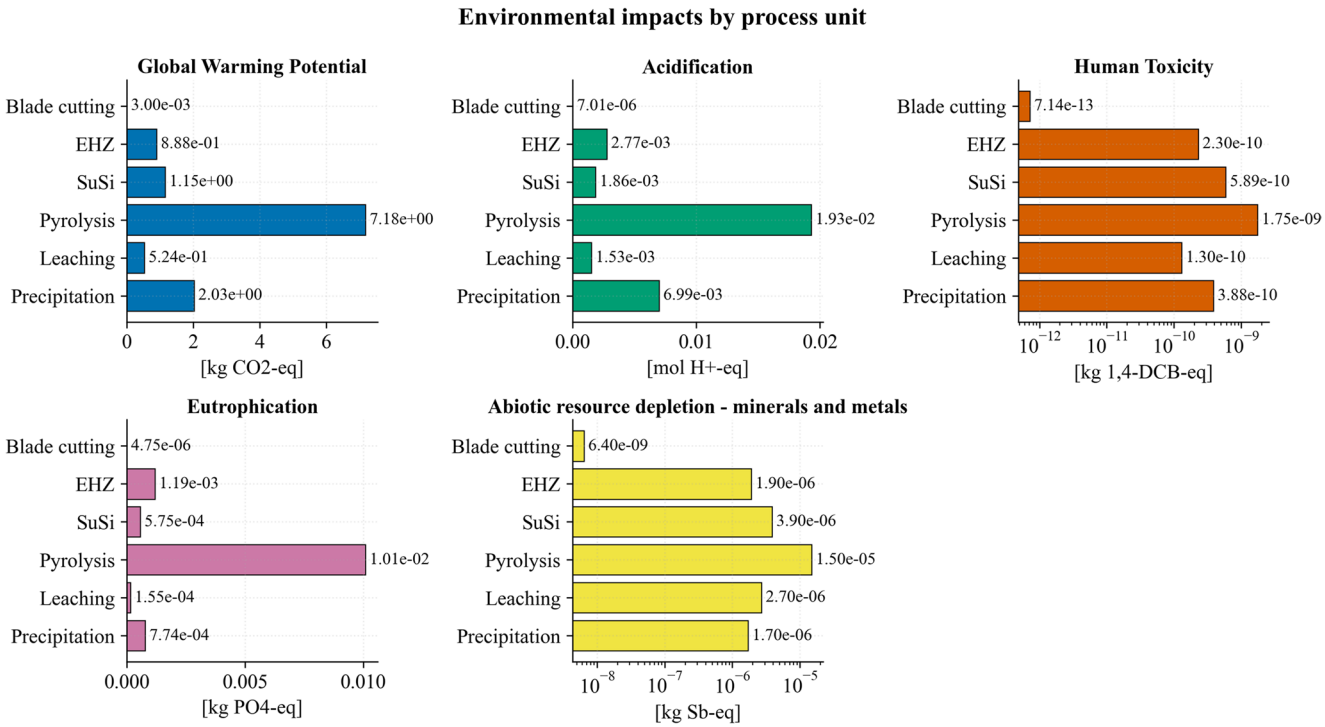

Fig. 8 LCA results for Global Warming Potential (kg CO_2-eq), Acidification (mol H^+-eq), Human Toxicity (kg 1,4-DCB-eq), Eutrophication (kg PO_4-eq), and Abiotic Resource Depletion of minerals and metals (kg Sb-eq)

d) **Identify and minimize the use of materials that will cause losses and contamination**: The Metal Wheel diagram proposed by [34] serves as a comprehensive tool for assessing the expected losses in various recovery routes tailored for NMC811 battery cells. This diagram not only highlights the potential losses associated with each recovery pathway but also emphasizes the importance of selecting appropriate routes to mitigate these losses effectively. In this context, when choosing a specific recovery route, it is anticipated that there will be inherent losses. This study, therefore, underscores the significance of avoiding the combination of incompatible materials during the recycling process. By integrating these considerations, stakeholders can make informed decisions aimed at optimizing recovery efficiency while minimizing resource wastage and environmental impact. The losses observed in the chosen metallurgical recovery route are consistent with the metallurgical wheel, indicating that different materials are incompatible when processed together. Nevertheless, it doesn't indicate process efficiency.

e) **Design cluster or subunits in products that can be easily removed and that match with the final treatment**: Unifying parts or designing clusters for processing can significantly enhance recovery rates by reducing contamination within the process. However, this approach necessitates achieving a high liberation rate. Processing the anode and cathode together is expected to result in inevitable losses. This strategy underscores the importance of targeted material recovery to improve overall efficiency and reduce waste in the recycling process.

f) **Label**: As shown in Fig. 6, a recycling label has been developed to indicate the total recovery of materials after the recycling process. This label provides a clear indication of the product's efficiency or inefficiency in terms of recyclability. By showcasing the effectiveness of the recycling process, the label serves as a valuable tool for assessing the sustainability and environmental impact of the product.

5.3 Life Cycle Assessment Results

Figure 8 shows the environmental impacts of each processing stage across five categories: Global Warming Potential (kg CO_2-eq), Acidification (mol H^+-eq), Human Toxicity (kg 1,4-DCB-eq), Eutrophication (kg PO_4-eq), and Abiotic Resource Depletion (kg Sb-eq). The results, covering the stages from cell cutting to lithium precipitation, highlight the relative contribution of each process and enable the identification of environmental hotspots for targeted optimization.

5.4 Design for Recycling Recommendations

Although the cell design developed and used in this project is based on sustainability criteria, there is still room for improvement. By analyzing the recycling process optimized for the general design of these battery cells, key design factors influencing the required process steps and their efficiency can be identified. A systematic evaluation of these factors enables the proposal of design modifications with significant potential to enhance material recovery, reduce process complexity, and lower environmental impacts.

The Anode and Cathode Liberation Designing the battery cell with an easily dismountable casing would allow for the direct processing of the anode, cathode, separator foil, and electrolyte in a pyrolysis unit, yielding significant environmental benefits after a single initial step. This design modification results in a 17% reduction in Global Warming Potential (GWP), a 14% reduction in acidification, a 26% reduction in Human Toxicity, and a 13% reduction in eutrophication impact categories. Such a design facilitates more efficient and environmentally friendly recycling processes by enabling easier access to critical components.

The Binder Traditional binders like polyvinylidene fluoride (PVDF) are soluble in a limited range of solvents, which can complicate the recycling process. Alternative binders that can disperse in water, such as carboxymethyl cellulose (CMC) or styrene–butadiene rubber (SBR), present distinct advantages. PVDF's mechanical properties, such as hardness and modulus of elasticity, deteriorate with age, negatively impacting the electrode's adhesiveness to the active material. Exploring binders that do not require solvents or even electrodes that forgo binders altogether could enhance recycling efficiency and material recovery.

The Electrolyte Fluorine-containing components in used batteries introduce additional processing complexities. Incorporating a fluoride precipitation unit necessitates the use of more reagents, complicating the recycling process. Therefore, a defluorination of LIBs would be highly beneficial. Implementing this approach would allow to remove that step from the recycling process and thus result in a 19% reduction in GWP, a 15% reduction in Acidification, a 27% reduction in Human Toxicity, and a 14% reduction in Eutrophication of the recycling process and thereby significantly improving the environmental footprint. Further one could think of improvements of the recycling process that might require design changes.

Delamination Separating the anode and cathode foil during recycling can prevent copper (Cu) and aluminum (Al) from becoming contaminants in hydrometallurgical processes. For example, aluminum foils are susceptible to oxidation and corrosion, which can introduce impurities during a froth flotation process used for active particle separation. Including a delamination process unit before physical and chemical processing could, according to the model, enhance the recycling index from 59% to 71%, ensuring cleaner and more efficient material recovery. Literature reports delamination efficiencies exceeding 99% for ultrasonic, water-based methods using mild reagents [47, 48]. Although direct comparison with the EHF route is limited by differing process maturity, this highlights opportunities for future process integration. A delamination unit was not tested in this project. To ensure effective delamination performance, it may be necessary to incorporate surface modifiers that facilitate delamination during the design phase.

Before Dismantling Proper discharge procedures are crucial to avoid undesirable side reactions, such as anode dissolution into the electrolyte and the formation of copper dendrites, which can contaminate material streams, including the cathode. Low-voltage cells should be discharged using a salt solution like NaCl or KCl to mitigate these issues, thereby ensuring the integrity of the recycling process. Design modifications at the cell level, including charge indicators or sub-cell discharging contacts, as well as process-related measures such as clearly defined discharging procedures, could enhance the safe discharge of cells prior to recycling. However, the impact of these modifications cannot be quantitatively assessed within the scope of this study due to the absence of data regarding process performance with partially charged cells and the projected prevalence of such cells in the recycling stream.

Before Leaching Incorporating a froth flotation process for active particle separation after implementing these recommendations can significantly enhance material recovery [35]. This process facilitates the separation of carbon (C) from the black mass, increasing the recovery of anode material and boosting the recycling index to 90%. In this scenario, it is crucial to use an alternative binder type, as the binder used in the anode can reharden after pyrolysis, leading to the formation of non-selective agglomerates. This consideration is essential for optimizing the recycling process and ensuring the highest possible material recovery rates.

6 Conclusion

Prioritizing sustainability in lithium-ion battery design greatly enhances their recyclability. Easily dismountable casings enable direct processing of key components, achieving a 19% reduction in Global Warming Potential

and substantial decreases in Acidification, Human Toxicity, and Eutrophication. Utilizing water-dispersible binders and eliminating fluorine in electrolytes simplify recycling and lower toxicity. Implementing a delamination step improves material purity and increases the recycling index from 59% to 71%, while proper discharge procedures and froth flotation can boost recovery rates to 90%. Several design improvements however are only effective, when the recycling process is applied exclusively to the improved design and adapted accordingly. Design for recycling and design for sustainability aren't just about product design; they also necessitate examining the design of all related processes, such as collection and recycling. These sustainable design principles and optimized recycling steps facilitate a circular economy for lithium-ion batteries, minimizing resource use and environmental harm while maximizing material recovery and recyclability. Based on these considerations, it is concluded that minor design modifications and further integrated optimization of both the design and recycling processes could substantially enhance the overall life cycle performance of the system through a systematic design-for-recycling approach, including targeted improvements within individual process units.

Acknowledgements This research was supported by HydroLiBRec (Optimierte Prozessketten für hydromechanisches Li-Ionen-Batterie-Recycling) project. The HydroLiBRec was funded by German Ministry of Education and Research (grant number: 03XP0339B). The authors is grateful to GRS Service GmbH and Robert Bosch GmbH for providing the input materials. Felipe Alejandro Garcia Paz would like to express his gratitude for the support provided by the Deutsche Forschungsgemeinschaft (DFG, German Research Foundation), funded by Project Number 461482547 (GRK 2802 – P11). The authors also thank Johannes Woth, Daniel Horn, Fabian Brückner and Axel Fabian (Fraunhofer IWKS) for their support during discharging, manual dismantling and EHF processing.

Funding Open Access funding enabled and organized by Projekt DEAL.

Declarations

Conflict of interest The authors declare no competing interests.

References

1. Nitta N, Wu F, Lee JT, Yushin G (2015) Li-ion battery materials: present and future. Mater Today. https://doi.org/10.1016/j.mattod.2014.10.040
2. Gao Z-W, Lan T, Yin H, Liu Y (2025) Development and commercial application of lithium-ion batteries in electric vehicles: a review. Processes 13(3):756. https://doi.org/10.3390/pr13030756
3. Thompson DL et al (2020) The importance of design in lithium ion battery recycling – a critical review. Green Chem 22:7585–7603. https://doi.org/10.1039/D0GC02745F
4. He B et al (2024) A comprehensive review of lithium-ion battery (LiB) recycling technologies and industrial market trend insights. Recycling 9(1):9. https://doi.org/10.3390/recycling9010009
5. European (2024) Critical Raw Materials Act
6. Montana F et al (2024) Assessing critical raw materials and their supply risk in energy technologies—a literature review. Energies 18(1):86. https://doi.org/10.3390/en18010086
7. Mineral Commodity Summaries 2023 (2023) doi: 10.3133/mcs2023
8. Harper G et al (2019) Recycling lithium-ion batteries from electric vehicles. Nature 575(7781):75–86. https://doi.org/10.1038/s41586-019-1682-5
9. Biswal BK, Zhang B, Thi Minh Tran P, Zhang J, Balasubramanian R (2024) Recycling of spent lithium-ion batteries for a sustainable future: recent advancements. Chem Soc Rev 53(11):5552–5592. https://doi.org/10.1039/D3CS00898C
10. Marashli A, Al-Kassab AI, Gab-Allah DM, Shalby M, Salah A (2024) Numerical life cycle assessment of lithium ion battery, Li-NMC type, integrated with PV system. Results Eng 23:102489. https://doi.org/10.1016/j.rineng.2024.102489
11. Machala ML et al (2025) Life cycle comparison of industrial-scale lithium-ion battery recycling and mining supply chains. Nat Commun 16(1):988. https://doi.org/10.1038/s41467-025-56063-x
12. Gaines L (2018) Lithium-ion battery recycling processes: research towards a sustainable course. Sustain Mater Technol 17:e00068. https://doi.org/10.1016/j.susmat.2018.e00068
13. Chen H, Yang Y, Dong Z (2025) The effect of product design on recycling efficiency of lithium-ion batteries through structural equation modeling and life cycle assessment. Sci Rep 15(1):12352. https://doi.org/10.1038/s41598-025-87663-8
14. Mattia Gianvincenzi M, Marconi, Enrico M, Mosconi FT, Tarantino M (2024) Eco-design and battery regulation: strategies for sustainable lifecycle management. Circular Economy 2(3)
15. Perocillo YK, Pirard E, Léonard A (2025) Process simulation-based LCA: Li-ion battery recycling case study. Int J Life Cycle Assess. https://doi.org/10.1007/s11367-025-02478-z
16. Torrubia J, Parvez AM, Sajjad M, García Paz FA, van den Boogaart KG (2024) Recovery of copper from electronic waste: an energy transition approach to decarbonise the industry. J Clean Prod 485:144349. https://doi.org/10.1016/j.jclepro.2024.144349
17. He SW et al (2025) Conceptual process design and LCA evaluation of precious metals recovery from waste PCBs. J Sustain Metall 11(3):2728–2743. https://doi.org/10.1007/s40831-025-01150-y
18. Baum ZJ, Bird RE, Yu X, Ma J (2022) Lithium-ion battery recycling─overview of techniques and trends. ACS Energy Lett 7(2):712–719. https://doi.org/10.1021/acsenergylett.1c02602
19. Rehman S, Al-Greer M, Burn AS, Short M, Cui X (2025) High-volume battery recycling: technical review of challenges and future directions. Batteries 11(3):94. https://doi.org/10.3390/batteries11030094
20. Tembo PM, Dyer C, Subramanian V (2024) Lithium-ion battery recycling—a review of the material supply and policy

infrastructure. NPG Asia Mater 16(1):43. https://doi.org/10.1038/s41427-024-00562-8
21. Bai Y, Muralidharan N, Sun Y-K, Passerini S, Stanley Whittingham M, Belharouak I (2020) Energy and environmental aspects in recycling lithium-ion batteries: concept of battery identity global passport. Mater Today 41:304–315. https://doi.org/10.1016/j.mattod.2020.09.001
22. Zhang Y et al (2023) Complete metal recycling from lithium-ion batteries enabled by hydrogen evolution catalyst reconstruction. J Am Chem Soc 145(50):27740–27747. https://doi.org/10.1021/jacs.3c10188
23. Wang J et al (2024) Toward direct regeneration of spent lithium-ion batteries: a next-generation recycling method. Chem Rev 124(5):2839–2887. https://doi.org/10.1021/acs.chemrev.3c00884
24. Jena KK, AlFantazi A, Choi DS, Liao K, Mayyas A (2024) Recycling spent lithium ion batteries and separation of cathode active materials: structural stability, morphology regularity, and waste management. Ind Eng Chem Res 63(8):3483–3490. https://doi.org/10.1021/acs.iecr.3c03673
25. Greenbatt (2025) HydroLIBRec – optimized process chains for hydromechanical Li-ion battery recycling. Accessed: May 22, 2025. [Online]. Available: https://www.greenbatt-cluster.de/en/projects/hydrolibrec/
26. Xu C, Dai Q, Gaines L, Hu M, Tukker A, Steubing B (2020) Future material demand for automotive lithium-based batteries. Commun Mater 1(1):99. https://doi.org/10.1038/s43246-020-00095-x
27. Holzer A et al (2022) A combined hydro-mechanical and pyrometallurgical recycling approach to recover valuable metals from lithium-ion batteries avoiding lithium slagging. Batteries 9(1):15. https://doi.org/10.3390/batteries9010015
28. Öhl J, Horn D, Zimmermann J, Stauber R, Gutfleisch O (2019) Efficient process for Li-Ion battery recycling via electrohydraulic fragmentation. Mater Sci Forum 959:74–78. https://doi.org/10.4028/www.scientific.net/MSF.959.74
29. Stallmeister C, Friedrich B (2023) Holistic investigation of the inert thermal treatment of industrially shredded NMC 622 lithium-ion batteries and its influence on selective lithium recovery by water leaching. Metals 13(12):2000. https://doi.org/10.3390/met13122000
30. Gao W et al (2017) Lithium carbonate recovery from cathode scrap of spent lithium-ion battery: a closed-loop process. Environ Sci Technol 51(3):1662–1669. https://doi.org/10.1021/acs.est.6b03320
31. Liu X, Li S, Liu Y, Cao Y (2015) Formic acid: a versatile renewable reagent for green and sustainable chemical synthesis. Chin J Catal 36(9):1461–1475. https://doi.org/10.1016/S1872-2067(15)60861-0
32. Hou J et al (2022) A green closed-loop process for selective recycling of lithium from spent lithium-ion batteries. Green Chem 24:7049–7060. https://doi.org/10.1039/D2GC01811J
33. ecoinvent (2025) ecoinvent database. Accessed: May 22, 2025. [Online]. Available: https://ecoinvent.org/database/
34. Aromaa R, Rinne M, Lundström M (2022) Comparative life cycle assessment of hardmetal chemical recycling routes. ACS Sustain Chem Eng 10(31):10234–10242. https://doi.org/10.1021/acssuschemeng.2c01969
35. Aromaa R, Rinne M, Lundström M (2023) Life cycle assessment of tantalum and niobium recycling from hard metal scrap. ACS Sustain Chem Eng 11(41):14997–15005. https://doi.org/10.1021/acssuschemeng.3c03540
36. Mohr M, Peters JF, Baumann M, Weil M (2020) Toward a cell-chemistry specific life cycle assessment of lithium-ion battery recycling processes. J Ind Ecol 24(6):1310–1322. https://doi.org/10.1111/jiec.13021
37. Rinne M, Elomaa H, Porvali A, Lundström M (2021) Simulation-based life cycle assessment for hydrometallurgical recycling of mixed LIB and NiMH waste. Resour Conserv Recycl 170:105586. https://doi.org/10.1016/j.resconrec.2021.105586
38. Simone F, Fabrizio B, Valeria DL, Luca Z, Serenella S, Edward D (2018) Supporting information to the characterisation factors of recommended EF life cycle impact assessment methods. no. KJ-NA-29600-EN-N (online),KJ-NA-29600-EN-C (print), 2018, https://doi.org/10.2760/002447(online)10.2760/090552(print)
39. Liu K, Tan Q, Yu J, Wang M (2023) A global perspective on e-waste recycling. Circ Econ 2(1):100028. https://doi.org/10.1016/j.cec.2023.100028
40. Seier M, Roitner J, Archodoulaki V-M, Jones MP (2023) Design from recycling: overcoming barriers in regranulate use in a circular economy. Resour Conserv Recycl 196:107052. https://doi.org/10.1016/j.resconrec.2023.107052
41. Ramakrishna B. R. Seeram (2024) Handbook of Materials Circular Economy
42. van Schaik A, Reuter MA (2014) Material-Centric (Aluminum and Copper) and Product-Centric (Cars, WEEE, TV, Lamps, Batteries, Catalysts) Recycling and DfR Rules. Handbook of Recycling. Elsevier, pp 307–378. https://doi.org/10.1016/B978-0-12-396459-5.00022-2
43. Reuter MA, van Schaik A, Gediga J (2015) Simulation-based design for resource efficiency of metal production and recycling systems: cases - copper production and recycling, e-waste (LED lamps) and nickel pig iron. Int J Life Cycle Assess 20(5):671–693. https://doi.org/10.1007/s11367-015-0860-4
44. Ernst Worrell MAR (2014) Handbook of recycling: state-of-the-art for practitioners, analysts, and scientists (table of contents)
45. Maris E, Froelich D, Aoussat A, Naffrechoux E (2014) From Recycling to Eco-design. Handbook of Recycling. Elsevier, pp 421–427. https://doi.org/10.1016/B978-0-12-396459-5.00027-1
46. Felipe Alejandro GP, Tina P, Ashak P, Mahmud, van den B, Karl, Gerald (2024) Optimierte prozessketten für hydromechanisches li-ionen-batterie-recycling helmholtz-institut freiberg für ressourcentechnologie (HIF)
47. Lei C et al (2021) Lithium ion battery recycling using high-intensity ultrasonication. Green Chem 23(13):4710–4715. https://doi.org/10.1039/D1GC01623G
48. Marshall J, Gastol D, Sommerville R, Middleton B, Goodship V, Kendrick E (2020) Disassembly of Li ion cells—characterization and safety considerations of a recycling scheme. Metals 10(6):773. https://doi.org/10.3390/met10060773